

GBA-UBF : A Large-Scale and Fine-Grained Building Function Classification Dataset in the Greater Bay Area

Chunsong Chen[#], Yichen Hou[#], Huan Chen[#], Junlin Li, Rong Fu,

Qiushen Lai, Yiping Chen^{*}, Ting Han^{*}

School of Geospatial Engineering and Science, Sun Yat-sen University, Zhuhai, China

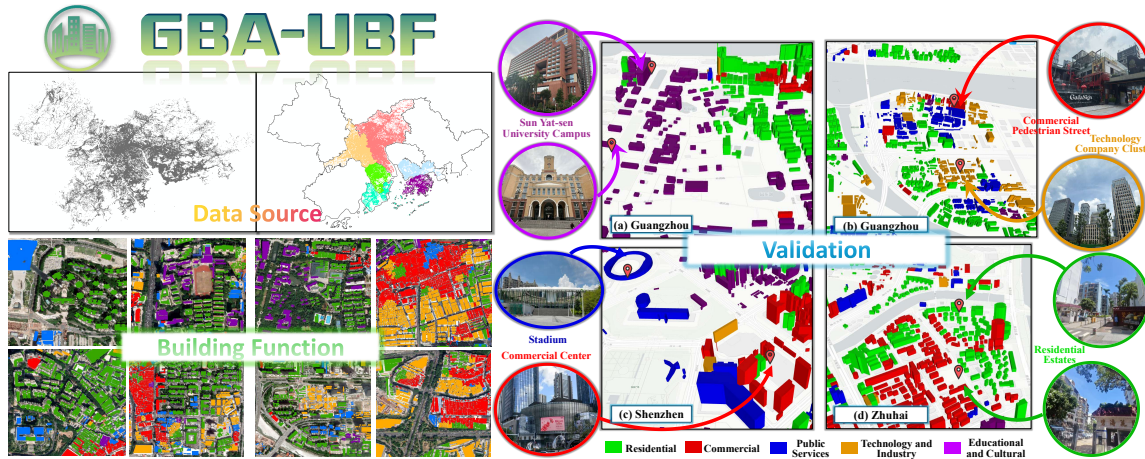


Figure 1: Overview of GBA-UBF Dataset, a building-level function dataset for the Greater Bay Area. GBA-UBF provides city-wide, building-scale labels that overcome the coarse granularity of parcel maps. It covers 4 million buildings across six core GBA cities with five unified classes: Residential, Commercial, Public Services, Technology & Industry, Educational & Cultural.

Abstract

Rapid urbanization in the Guangdong–Hong Kong–Macao Greater Bay Area (GBA) has created urgent demand for high-resolution, building-level functional data to support sustainable spatial planning. Existing land use datasets suffer from coarse granularity and difficulty in capturing intra-block heterogeneity. To this end, we present the **Greater Bay Area Urban Building Function Dataset (GBA-UBF)**, a large-scale, fine-grained dataset that assigns one of five functional categories to nearly four million buildings across six core GBA cities. We proposed a **Multi-level Building Function Optimization (ML-BFO)** method by integrating Points of Interest (POI) records and building footprints through a three-stage pipeline: (1) candidate label generation using spatial overlay with proximity weighting, (2) iterative refinement based on neighborhood label autocorrelation, and (3) function-related correction informed by High-level POI buffers. To quantitatively validate results, we design the Building Function Matching Index (BFMI), which

jointly measures categorical consistency and distributional similarity against POI-derived probability heatmaps. Comparative experiments demonstrate that GBA-UBF achieves significantly higher accuracy, with a BFMI of 0.58. This value markedly exceeds that of the baseline dataset and exhibits superior alignment with urban activity patterns. Field validation further confirms the dataset's semantic reliability and practical interpretability. The GBA-UBF dataset establishes a reproducible framework for building-level functional classification, bridging the gap between coarse land use maps and fine-grained urban analytics. The dataset is accessible at <https://github.com/chenchs0629/GBA-UBF>, and the data will undergo continuous improvement and updates based on feedback from the community.

CCS Concepts

• Information systems → Geographic information systems.

Keywords

Building Function Dataset, Urban Land Use, Points of Interest (POI), Greater Bay Area, Building Footprint

ACM Reference Format:

Chunsong Chen[#], Yichen Hou[#], Huan Chen[#], Junlin Li, Rong Fu, Qiushen Lai, Yiping Chen^{*}, Ting Han^{*}. 2025. GBA-UBF : A Large-Scale and Fine-Grained Building Function Classification Dataset in the Greater Bay Area. In *The 4th ACM SIGSPATIAL International Workshop on Spatial Big Data and AI for Industrial Applications (GeoIndustry '25)*, November 3–6, 2025, Minneapolis, MN, USA. ACM, New York, NY, USA, 12 pages. <https://doi.org/10.1145/3764919.3770875>

Permission to make digital or hard copies of all or part of this work for personal or classroom use is granted without fee provided that copies are not made or distributed for profit or commercial advantage and that copies bear this notice and the full citation on the first page. Copyrights for components of this work owned by others than the author(s) must be honored. Abstracting with credit is permitted. To copy otherwise, or republish, to post on servers or to redistribute to lists, requires prior specific permission and/or a fee. Request permissions from permissions@acm.org.

GeoIndustry '25, Minneapolis, MN, USA

© 2025 Copyright held by the owner/author(s). Publication rights licensed to ACM.

ACM ISBN 979-8-4007-2182-3/2025/11

<https://doi.org/10.1145/3764919.3770875>

1 Introduction

Accurate classification of urban land use and building functions plays a crucial role in spatial planning and sustainable development. Fine-grained functional mapping not only supports the optimization of urban spatial structures but also guides infrastructure deployment and enables evidence-based governance.

In recent years, the proliferation of social media and mobile internet has made user-generated content (UGC) an important geospatial data source. With its near real-time updates, broad coverage, and strong linkages to human activities, UGC complements traditional Earth observation (EO) datasets, such as high-resolution satellite imagery. For land-use inference, UGC enriches socio-economic semantics that are often missing in conventional EO products and supports refined functional zoning [35]. Prior studies that integrate UGC (e.g., Points of Interest (POI), GPS trajectories, and OpenStreetMap) with EO imagery have reported notable advances in urban land-use classification and functional mapping [5, 22, 39].

Nevertheless, mainstream land-use datasets remain parcel-based, where blocks are annotated with functions such as residential, commercial, industrial, public services, or green spaces. While parcel-level maps underpin critical planning tasks such as the delineation of Urban Functional Zones (UFZs) [17] and assessments of urban growth dynamics [31], they suffer from several limitations:

- (1) **Inconsistent classification standards.** heterogeneous taxonomies hinder benchmarking and validation.
- (2) **Inconsistent parcel delineation.** variations in road-based segmentation rules lead to spatial inconsistencies and scale effects [16].
- (3) **Multi-functionality and scale mismatch.** parcels often contain hundreds of buildings with mixed uses, undermining assumptions of homogeneity.

These limitations constrain the robustness and applicability of parcel-level data for fine-scale urban research.

Buildings, as the atomic units of cities, accommodate living, working, commerce, education, and recreation, thereby encoding fine-grained land use information [48]. Studies leveraging POI, remote sensing imagery, and UGC have demonstrated the potential of building-level functional inference [24, 36], enabling applications ranging from emergency response [30] and policy-making [46] to resource management [34].

Recent advances in spatiotemporal big data (e.g., Google Maps, Amap, and Baidu Maps) have also made large-scale building-level analysis feasible. POI datasets provide semantic attributes, while building footprints capture precise geometries, together offering unprecedented opportunities to move beyond coarse parcel-based datasets toward detailed, reproducible urban function mapping. However, existing research often remains limited to small-scale case studies, lacks standardized classification schemes, and rarely validates across cities with diverse morphologies.

Against this backdrop, the Guangdong–Hong Kong–Macao Greater Bay Area (GBA) emerges as a compelling context to address these research gaps. China released the Outline Development Plan for the GBA in 2019, which set forth the strategic goal of developing the GBA into a world-class bay area. Among the world's four major bay areas, the GBA is the largest in land area, population, and industrial agglomeration, thereby facing highly complex challenges

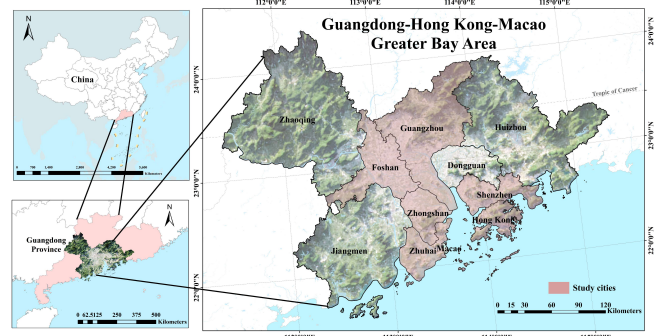


Figure 2: Geographical Location of the GBA and Study Area.

in urban planning, demographic dynamics, human activities, and community infrastructure [19]. Given the GBA's extreme population density, diverse economic activities, and fragmented urban expansion, traditional land-cover mapping alone is insufficient. Consequently, building-level functional classification is essential for formulating responsive policies and adaptive urban management. Meanwhile, the GBA comprises 11 cities or special administrative regions with distinct urban forms and industries, making an urban building function dataset built upon this urban agglomeration both representative and unique.

However, there remains no large-scale, fine-grained building function dataset for the GBA. To fill this gap, this study constructs the new **Greater Bay Area Urban Building Function Dataset (GBA-UBF)**, which covers nearly four million buildings across six core cities. The dataset is generated through a reproducible three-stage pipeline, which we have named as **Multi-level Building Function Optimization (ML-BFO)** method: (1) Candidate label generation via spatial overlay of POI and building footprints with proximity-weighted scoring. (2) Iterative refinement leveraging neighborhood label autocorrelation to enhance spatial consistency. (3) Function-related correction incorporating advanced POI buffers to capture the influence of landmark facilities.

We further propose the Building Function Matching Index (BFMI), a novel evaluation metric that integrates categorical consistency with distributional similarity against POI probability heatmaps. Comparative analysis with the EULUC-China 2.0 dataset demonstrates the superior granularity and accuracy of GBA-UBF, particularly in high-density and mixed-use areas. Field validation confirms its semantic reliability and practical interpretability.

2 Related works

2.1 Urban Land Use Dataset

Land use and land cover (LULC) mapping is foundational to urban and regional planning and is now a core enabler of smart, sustainable cities [1]. Recent advances in very-high-resolution (VHR) Earth observation, together with the rapid expansion and cross-domain integration of multimodal geospatial data, have produced a new generation of LULC products that are spatially explicit, temporally consistent, and operational at scale. The representative datasets include GlobalLand30 [6], FROM-GLC30 and FROM-GLC10 [13, 14], the ESA WorldCover (10 m) suite [42], GLC-FCS10 (10 m) derived from Sentinel imagery on Google Earth Engine [45], 3-m national

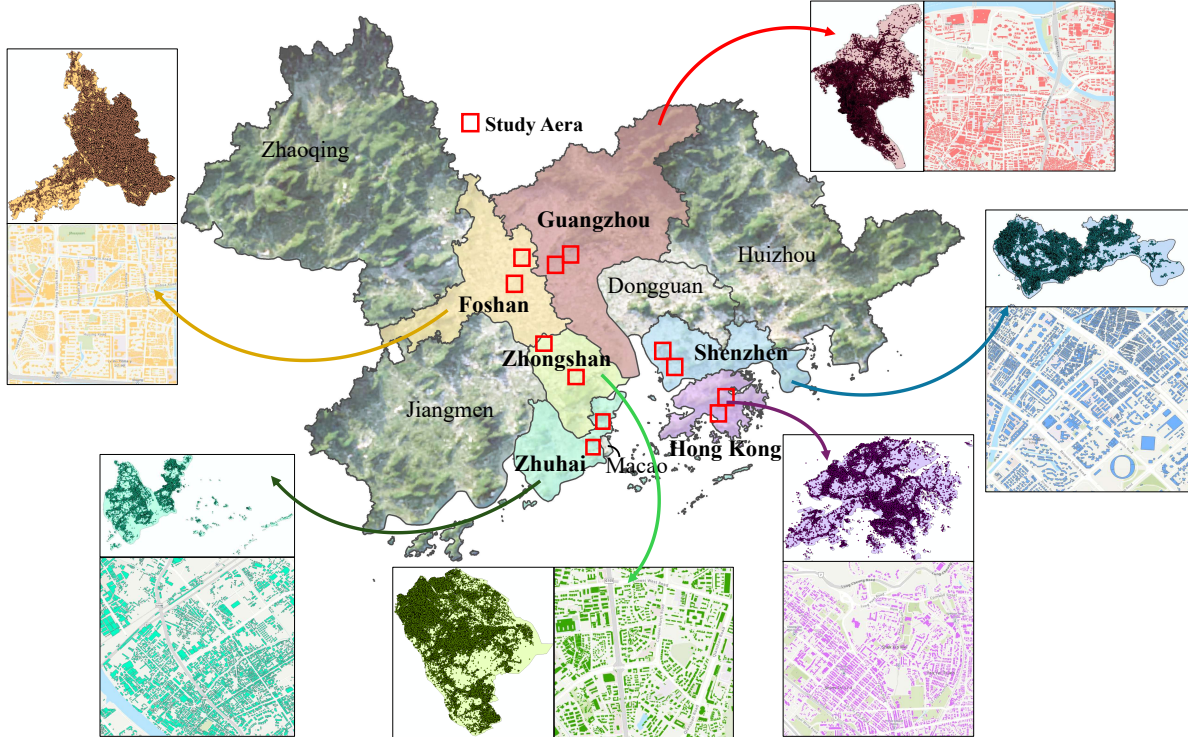


Figure 3: Location and Data Overview of the Study Area within the Greater Bay Area. Different colors represent different cities, and for each city we show both the distribution of POI and representative building footprints.

maps of China generated using public 10-m land cover maps as training data [10], and the SinoLC-1 (1 m) product [23]. These products exemplify the field's shift toward higher spatial resolution and more frequent updates in global LULC mapping.

In contrast, urban land use (ULU) is substantially harder to delineate than land cover due to semantic ambiguity, temporal volatility, and pervasive mixed use. The intensification of human-driven land transformation makes accurate, intra-urban ULU characterization scientifically important and operationally urgent. High-resolution Earth observation provides the spatial detail and radiometric quality required for fine-scale ULU mapping [15]. Over the past decade, methodological advances have systematically exploited textural, geometric, and contextual cues in these data, yielding increasingly discriminative representations of urban form and function, from object-based image analysis to deep context modeling [3, 9, 33].

However, spectral-only classification quickly reaches the information ceiling of imagery and cannot deliver the granularity demanded by complex urban scenes. The proliferation of spatiotemporal big data and social sensing has enriched land-use representations and enabled more refined mapping. OpenStreetMap (OSM) is widely used to regularize labels and improve classification [12, 40]. However, its inherent incompleteness and positional uncertainty remain non-trivial constraints [47]. UGC enables crowdsourced, continuously updated, activity-aware geospatial datasets [37]. In particular, points of interest (POI) supply semantic labels largely absent from Earth-observation imagery, providing supervision/weak supervision and reference annotations for urban land-use classification [27, 38]. Fusing POI-derived features with VHR imagery and

OSM consistently yields more accurate and more robust land use maps [2, 26, 39].

2.2 Urban Building Function Analysis

Urban Functional Zoning (UFZ) refers to the division of urban areas into zones according to their dominant functions, such as residential, commercial, industrial, and public service areas. With the acceleration of global urbanization, the accurate identification of UFZs is critical for optimizing urban spatial structure, guiding planning, and improving resource allocation [25]. Traditional functional zoning has relied primarily on land-use planning maps and census data, which suffer from long update cycles and coarse resolution, limiting their ability to capture rapidly changing urban morphologies.

With the widespread adoption of Geographic Information Systems, remote sensing, and location-based services, researchers have increasingly turned to spatial big data for UFZ identification. Among these, POI provide rich semantic features that offer fine-grained descriptions of urban functions, making POI-based methods a major research focus. Many studies have employed POI spatial distributions and categorical attributes, often combined with kernel density estimation, clustering, or other statistical methods, to delineate UFZs and reveal their spatial patterns [28].

For instance, Zhang et al. [44] automatically delineated the functional zones of Hangzhou using POI data, while Miao et al. [29] extracted urban spatial patterns from Sina Weibo POI. Hong et al. [18] highlighted the role of roads in shaping functional distributions by integrating POI data with OpenStreetMap. Beyond single-source

Table 1: Comparative Statistics of POI Quantity and Building Footprints in Selected Cities' study areas.

City	POI Quantity	Building Footprints
Guangzhou	1,499,128	1,351,299
Shenzhen	1,413,510	741,612
Zhongshan	404,371	391,665
Zhuhai	183,090	171,031
Foshan	771,242	1,038,253
Hong Kong	546,720	175,905

Table 2: Correspondence between Building Function Types and Baidu POI Classification.

Building Function Type	Baidu POI Primary Classification System
Residential	Real Estate
Commercial	Food, Hotel, Shopping, Life Services, Beauty Services, Recreation Center, Sports and Fitness Center, Car Services, Financial Industry
Public Services	Life Services, Culture and Media, Government Agencies, Transportation, Healthcare, Tourist Attractions
Technology and Industry	Companies and Enterprises
Educational and Cultural	Education and Training Venue

approaches, the integration of multi-source data has further advanced UFZ research. Zhang et al. [43] proposed a hierarchical semantic framework that fused very-high-resolution (VHR) imagery with POI, while Liu et al. [26] combined Landsat imagery with taxi GPS and POI to recognize UFZs. These studies collectively demonstrate the potential of fusing multi-source spatial and semantic data to improve the accuracy and interpretability of UFZ identification across different urban scales and contexts.

3 Dataset and Study Area

3.1 Study Area

The Guangdong–Hong Kong–Macao Greater Bay Area (GBA), anchored in the Pearl River Delta, spans 56,000 km² and is home to over 86 million residents, making it one of China's most urbanized and densely populated regions. The GBA includes nine Guangdong prefectures: Guangzhou, Shenzhen, Zhuhai, Foshan, Zhongshan, Dongguan, Huizhou, Jiangmen, Zhaoqing—as well as the Hong Kong and Macao Special Administrative Regions (SARs).

In terms of functional specialization, Shenzhen is positioned as the innovation hub, Guangzhou as the integrated services and transport gateway, Hong Kong as the global financial and shipping center, Macao as a world tourism and leisure hub, and the Dongguan and Foshan area as a center for advanced manufacturing. With seamless transport connectivity envisioned to link these key nodes into a high-productivity megalopolis, the GBA faces significant governance challenges in coordinating a nearly 100 million strong, polycentric region with overlapping jurisdictions. The geographic extent of the GBA is shown in Fig. 2.

Urbanization in the GBA is well advanced, but ongoing integration is blurring inter-city boundaries and accelerating the urbanization of peri-core areas. Shenzhen (density >7,000 inhab/km²) and Guangzhou (density >2,000 inhab/km²) exemplify extreme urban density and intensifying mixed land use [32]. The functional distinctions between municipalities are becoming less clear, making

traditional administrative zoning inadequate for coordinated governance and efficient resource allocation. Additionally, the varying development stages and functional mandates across cities lead to diverse spatial distributions of residential, commercial, industrial, technological, public service, and educational facilities.

To address this complexity, the study focuses on the central urban areas of six cities—Guangzhou, Shenzhen, Hong Kong, Zhuhai, Zhongshan, and Foshan—chosen for data availability, analytical feasibility, and structural comparability. Guangzhou and Shenzhen represent the traditional urban core and innovation-driven metropolis, respectively, while Hong Kong exemplifies compact vertical urbanism. Foshan and Zhongshan are characterized by manufacturing-focused zoning, and Zhuhai offers a tourism-oriented, livable morphology. These cities span various urban tiers, ensuring the dataset's representativeness and cross-city comparability. The study area location within the GBA and data overview are presented in Fig. 3.

3.2 Data Sources

To support urban functional analysis, we integrate two complementary data sources:

- **Building Footprints:** Aggregated from Baidu Maps¹ and OSM². We unify the data formats, remove duplicate polygons, and reproject all geometries, yielding accurate building footprints for further analysis.
- **POI Data:** POIs are sourced from Baidu Maps. Each POI provides a georeferenced location and rich attributes (name, address, category), enabling inference of urban building functions. As curated records of real-world entities on a high-traffic commercial platform, Baidu POI serve as timely, activity-aware proxies for land use in China. For functional labeling, we parse the Baidu industrial-type field into primary and secondary categories and harmonize it to a 19-class primary taxonomy adopted in this paper.

The quantity of POI and building footprints for each city's study areas is summarized in Tab. 1.

3.3 POI Reclassification with Building Function

Baidu POI data consist of 19 primary categories³. For the purpose of building function identification, we manually exclude three non-building categories: entrances/exits, roads, and natural features. To improve the accuracy of delineating urban spatial structure, and following the National Standard for Urban Land Use and Planning (GB 50137-2011), we further remove land-use types that lack physical buildings and consolidate the remaining categories. As a result, all urban buildings are classified into five functional types: Commercial Services, Residential, Technology and Industry, Educational and Cultural, and Public Services.

Tab. 2 lists each functional type and its corresponding POI sub-categories. Specifically, Commercial Services encompass daily commercial premises supporting business and consumption; Public Services include government, healthcare, transportation, cultural,

¹<https://map.baidu.com/>

²<https://www.openstreetmap.org/>

³dining, hotels, shopping, life services, beauty services, tourist attractions, leisure and entertainment, sports and fitness, education and training, culture and media, medical care, cycling services, transportation facilities, finance, real estate, companies and enterprises, government agencies, entrances/exits, and natural features

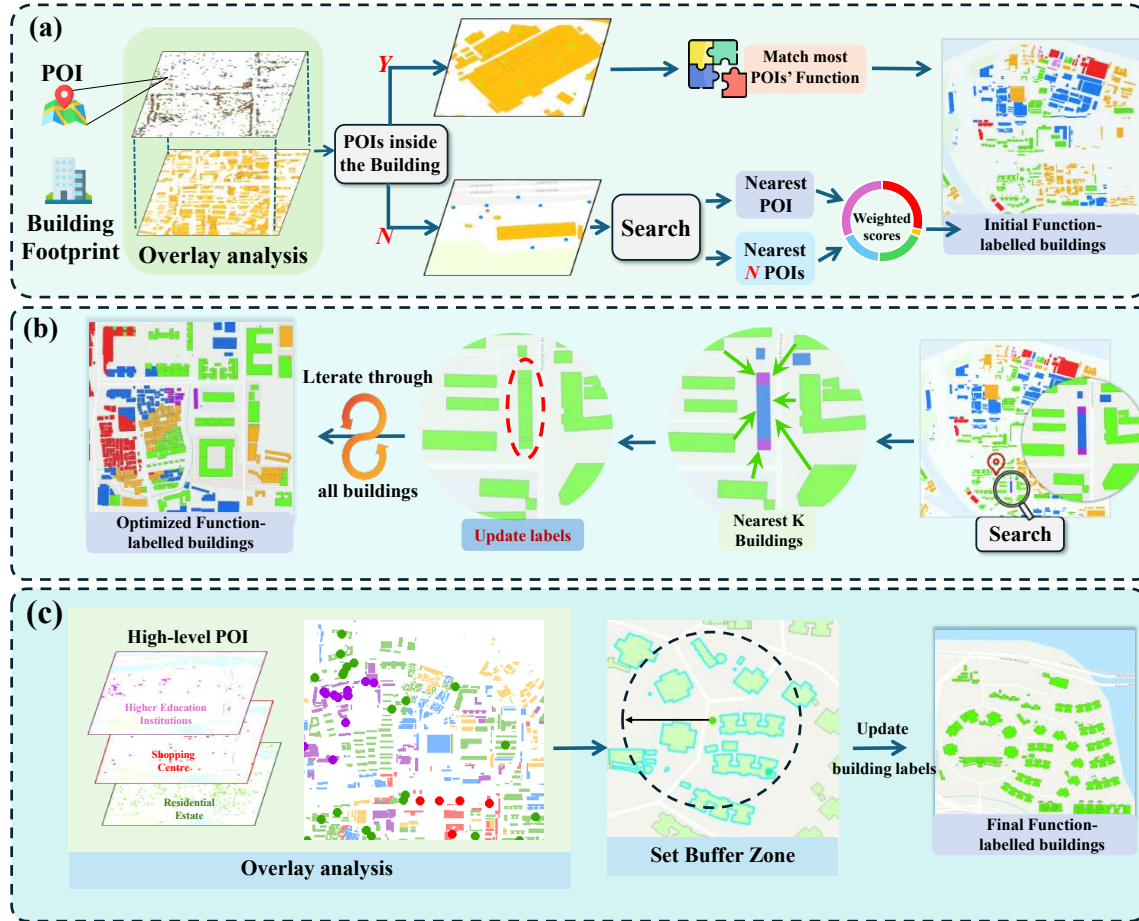


Figure 4: Overall of dataset generation framework. We use a reproducible 3-stage pipeline: (a) Candidate Function Label Generation; (b) Iterative Label Distribution Refinement; and (c) Function Related Label Correction.

and public facilities; Residential refers to dwelling-oriented areas; Technology and Industry cover science parks, industrial estates, factories, and office complexes; and Educational and Cultural represent schools, universities, and research institutes.

This taxonomy is grounded in theories of urban land use and functional zoning, integrating POI attributes with spatial distribution patterns to capture the dominant socio-economic role of each building. In practice, buildings often exhibit mixed functions, such as retail stores embedded in residential compounds. However, this dataset does not include a mixed-use category, as the complexity of such classification greatly increases annotation difficulty, and scholarly consensus on its definition remains limited [11]. Adopting a dominant-function strategy ensures classification stability, reproducibility, and comparability across cities.

4 Methodology

In this study, we proposed a **Multi-level Building Function Optimization (ML-BFO)** method. It consists of three core stages: (1) **Candidate function label generation**; (2) **Iterative label distribution refinement**; and (3) **Function-related label correction**, as shown in Fig. 4. Moreover, we further design the **Building**

Function Matching Index (BFMI) to quantitatively assess the reliability of the dataset. The details are as follows.

4.1 Candidate Function Label Generation

In large-scale urban spatial analysis, accurately identifying and labeling the functional attributes of buildings is essential for understanding urban structure and dynamics. Due to the high density and large volume of POI data provided by Baidu Maps, which far exceed the number of building footprints, we propose a candidate function label generation method via spatial overlay representation.

Let a building B_i contain the POI set $\mathcal{P}_i = \{p_{i1}, p_{i2}, \dots, p_{in}\}$, where each POI p_{ij} belongs to a category $c(p_{ij}) \in C$, $C = \{1, 2, 3, 4, 5\}$.

Spatial proximity score. To quantify the spatial relevance between a POI and its nearby building, we define a *spatial proximity score* as:

$$\alpha_{ij} = \frac{1}{1 + d(p_{ij}, B_i)}, \quad (1)$$

where $d(p_{ij}, B_i)$ denotes the shortest Euclidean distance between POI p_{ij} and the boundary of building B_i . A smaller distance implies that the POI is more closely associated with the building—either functionally or spatially—indicating a higher likelihood that the

POI's category reflects the building's actual use. Conversely, distant POIs have weaker spatial linkage and thus contribute less to the functional label.

Category-specific weight. Since the frequency of different POI categories varies across study aera, the importance of each category is further modulated by a *category-specific weight* $w_c(B)$, which reflects the relative representativeness of category c within the local block B . For each block B , we compute the category count $\text{freq}_c(B)$ and the total number of POIs $N(B)$. The weight is defined with a power decay function as:

$$w_c(B) = \frac{1}{(\text{freq}_c(B) + 1)^\alpha}, \quad \alpha \in [0.3, 1.0]. \quad (2)$$

This formulation reduces the dominance of highly frequent categories while preserving the contribution of rare but strongly indicative POIs. The parameter α is manually set based on different study areas.

Composite score and label assignment. The composite score of building B_i for category c is computed as:

$$S_i(c) = \sum_{p_{ij} \in \mathcal{P}_i, c(p_{ij})=c} w_c(B) \cdot \alpha_{ij}. \quad (3)$$

Finally, the dominant functional label is assigned according to the maximum score:

$$L_i = \arg \max_{c \in C} S_i(c). \quad (4)$$

This method generates stable candidate labels and provides a robust basis for subsequent refinement.

4.2 Iterative Label Distribution Refinement

The initial POI-derived building labels may be noisy, especially in mixed-use or data-sparse areas. To improve label accuracy and robustness, we introduce an iterative refinement strategy based on spatial autocorrelation, leveraging the assumption that nearby buildings tend to share similar functions.

Formally, let the building set be $B = \{b_1, b_2, \dots, b_n\}$ with initial labels $L^{(0)}(b_i)$. For each building b_i , denote its k nearest neighbors as $N_k(b_i)$. At iteration t , the label update rule is defined as:

$$L_i^{(t+1)} = \begin{cases} \arg \max_{l \in \mathcal{L}} \sum_{j \in N_k(i)} \mathbf{1}(L_j^{(t)} = l), & \text{if } \Phi_i^{(t)} > \frac{k}{2}, \\ L_i^{(t)}, & \text{otherwise.} \end{cases} \quad (5)$$

where $\Phi_i^{(t)} = \max_{l \in \mathcal{L}} \sum_{j \in N_k(i)} \mathbf{1}(L_j^{(t)} = l)$ denotes the maximum count of label l among the k neighbors of building b_i .

This process repeats until convergence (no significant label changes) or until a preset maximum number of iterations is reached. By integrating neighborhood label distributions, the method enhances local consistency, reinforces spatial clustering, and significantly improves the precision of urban functional zoning.

4.3 Function Related Label Correction

To further enhance label accuracy, we propose a correction mechanism that integrates High-level POI and their surrounding buffer zones. High-level POI are defined as landmark facilities with strong functional implications, such as large commercial centers, residential complexes, and higher-education institutions. These facilities

not only determine the function of the buildings they occupy but also exert influence on the surrounding urban fabric. To capture this effect, we generate buffers of varying radii for each High-level POI, representing its spatial sphere of influence.

During the correction phase, each building with an initial label is examined against these High-level POI buffers. If a building falls within the buffer of a given POI, its label is updated to match the category of POI, reflecting its functional association. For instance, a building initially labeled as "Residential" may be reclassified as "Commercial" if it lies within the buffer of a large shopping mall. By leveraging the radiating effects of landmark facilities, this method introduces higher-level semantic correction, improving both the accuracy and granularity of functional zoning.

4.4 Evaluation Metric System Design

To assess the accuracy of the derived urban building function classifications, we introduce the **Building Function Matching Index (BFMI)**. Considering the lack of reliable ground-truth data and the fact that existing land-use datasets cannot capture the fine-grained characteristics of building-level functional patterns, traditional evaluation metrics (e.g., precision, recall, F1-score) are not directly applicable. Therefore, BFMI provides a practical alternative for quantitative evaluation. It quantitatively measures the alignment between building-level classification outcomes and POI-derived spatial probability distributions.

4.4.1 POI Probability Heat Map Generation. Specifically, POI records corresponding to the five functional categories are processed using Kernel Density Estimation (KDE) to generate class-specific heat maps. These heat maps serve as reference standards, capturing the spatial clustering and distributional characteristics of each functional type. For each functional class $c \in \{1, \dots, 5\}$, KDE is applied to the raw POI to obtain the density function $D_c(x)$. Then, we apply a softmax transformation to derive normalized probability surfaces:

$$P_{\text{poi},c}(x) = \frac{D_c(x)}{\sum_{k=1}^5 D_k(x) + \epsilon}, \quad (6)$$

where ϵ is a smoothing term.

4.4.2 Reference Label Approximation. For each building polygon B_i , we extract pixel values from the POI-based probability raster within its footprint and compute zonal statistics. By averaging across the polygon, we obtain a probability distribution vector over the five functional classes:

$$\bar{P}_{\text{poi}}(B_i) = (\bar{p}_1, \bar{p}_2, \dots, \bar{p}_5), \quad \sum_{c=1}^5 \bar{p}_c = 1, \quad (7)$$

where \bar{p}_c represents the average probability that building B_i belongs to functional class c , reflecting the predictive tendency derived from the POI raster.

Meanwhile, the approximation label y_i of building B_i is encoded as a one-hot vector:

$$P_{\text{bld}}(B_i) = \text{one_hot}(y_i). \quad (8)$$

For example, if building B_i is Residential, the corresponding one-hot vector is $(0, 1, 0, 0, 0)$. This encoding enables direct vector space comparison between the true building label and the POI-derived probability distribution.

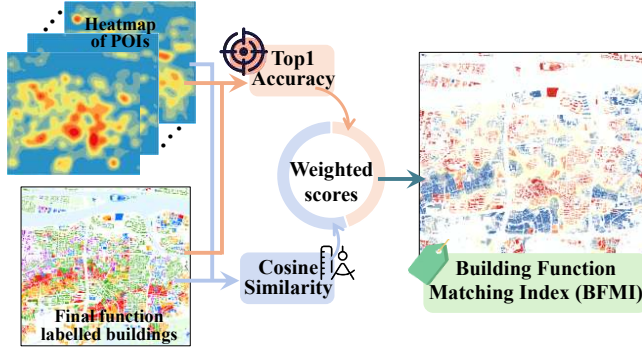


Figure 5: Construction of the Building Function Matching Index (BFMI). POI records are converted to class-specific KDE heatmaps and compared with the final building-level labels. For each building we compute (1) Top-1 Consistency with the dominant POI class and (2) Cosine Similarity between the one-hot label and the POI-derived probability vector, to generate the BFMI score map.

4.4.3 Evaluation Metrics. Ours BFMI integrates categorical accuracy and distributional consistency, as shown in Fig. 5. For each building B_i , two components are computed:

(a) Top-1 Consistency. This metric checks whether the predicted functional class matches the reference label:

$$\text{Top1}(B_i) = \mathbb{1}\{\arg \max_c \hat{p}_c = y_i\}, \quad (9)$$

where \hat{p}_c denotes the predicted probability for class c , and y_i is the reference class of building B_i .

(b) Distributional Similarity. To measure alignment between the predicted probabilities and the POI-derived reference distribution, we adopt cosine similarity:

$$\text{Cos}(B_i) = \frac{\bar{P}_{\text{poi}} \cdot P_{\text{bld}}}{\|\bar{P}_{\text{poi}}\| \|P_{\text{bld}}\|} = \frac{\bar{P}_{y_i}}{\sqrt{\sum_{c=1}^C \bar{p}_c^2}}, \quad (10)$$

where \bar{P}_{poi} is the POI-based probability vector and P_{bld} is the one-hot encoding of the predicted label. $\text{Cos}(B_i)$ ranges from 0 to 1, with higher values indicating stronger agreement between the prediction and the dominant POI distribution.

(c) Comprehensive Index (BFMI). Finally, the two components are fused into the BFMI:

$$\text{BFMI} = \frac{1}{N} \sum_{i=1}^N \left[w \cdot \text{Top1}(B_i) + (1 - w) \cdot \text{Cos}(B_i) \right], \quad (11)$$

where $w \in [0, 1]$ is a balancing weight. In this study we set $w = 0.5$ as default, giving equal importance to Top-1 consistency and cosine similarity.

5 Results and Discussion

5.1 Dataset Description

Our Greater Bay Area Urban Building Function (GBA-UBF) Dataset delineates five major building functions: **Commercial Services**, **Residential**, **Public Services**, **Technology and Industry**, and **Educational and Cultural**, as shown in Tab. 2. Each building

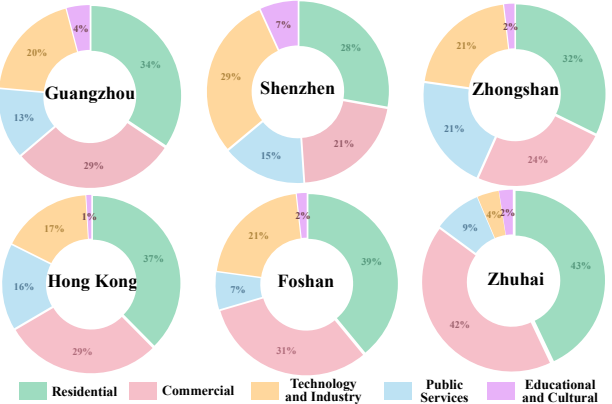


Figure 6: Distribution of Building Functional Categories in the Central Urban Areas of Six GBA Cities.

footprint is explicitly assigned to one functional category, ensuring a consistent and fine-grained representation of the urban built environment. Data compilation required half a year of effort by a five-member team, involving POI collection, footprint cleaning, algorithm refinement, and manual validation. To standardize processing, the dataset is first organized into five shapefiles and then merged into a unified geospatial layer with class attributes. Building footprints are stored at the polygon level, supporting precise delineation and detailed analyzes of function allocation and validation. The dataset also incorporates building-height attributes, enabling statistical assessment and spatial modeling.

In terms of file structure, each record contains the building geometry (polygon), functional class, spatial reference system, and exact geographic coordinates of vertices, ensuring compatibility with standard GIS workflows. The distribution of building function categories across the six cities is illustrated in Fig. 6. The dataset covers the central urban cores of six representative GBA cities: Guangzhou, Shenzhen, Hong Kong, Foshan, Zhongshan, and Zhuhai. For each city, two representative zones of approximately 5×5 km are selected for dataset construction. The processed areas include 45,000 buildings in Guangzhou, 38,000 in Shenzhen, 20,000 in Hong Kong, 69,000 in Foshan, 21,000 in Zhongshan, and 13,000 in Zhuhai, amounting to more than 300 km².

5.2 Qualitative Comparison

Compared with traditional land use datasets, building function datasets provide finer spatial resolution and higher descriptive accuracy. Conventional land use data are typically organized at the parcel and block level, with coarse granularity and ambiguous boundaries, making it difficult to capture intra-parcel heterogeneity and mixed-use patterns. In contrast, building function datasets are defined at the individual building scale, enabling a more precise representation of functional variations between structures and offering deeper insights into the fine-grained urban space. Moreover, they can integrate multiple data sources (e.g., POI, remote sensing imagery, statistical records), supporting dynamic updates and multidimensional representations.

The comparison between the *GBA-UBF Dataset* and the *EULUC-China* datasets [22] is shown in Fig. 7. The two EULUC products, while effective at capturing general land-use patterns, operate at the

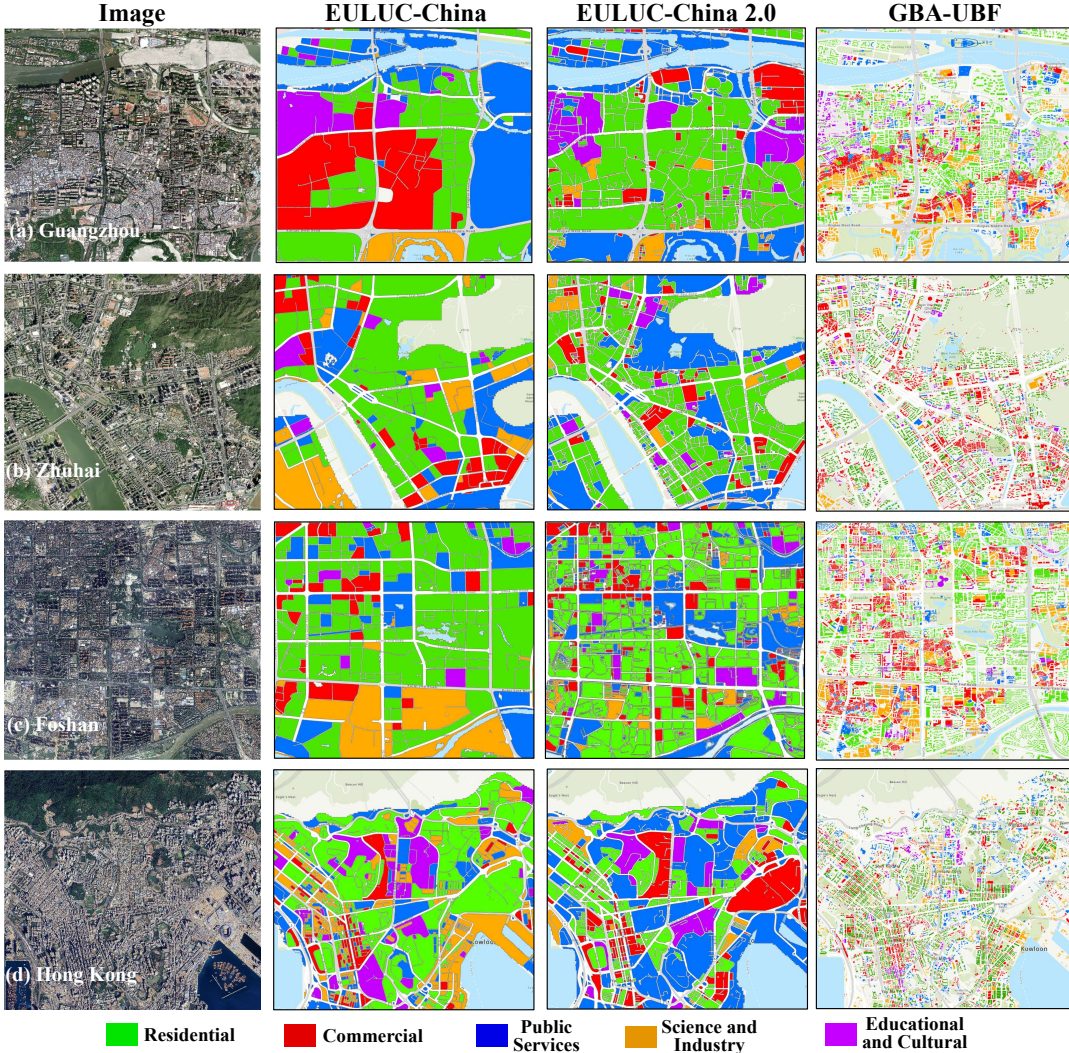


Figure 7: The Comparison between the GBA-UBF Dataset and EULUC-China Dataset.

parcel or block level, resulting in coarse boundaries and a limited ability to represent mixed-use structures. Functional heterogeneity within parcels is largely obscured, and many small-scale facilities are generalized into broader classes. In contrast, the GBA-UBF dataset defines functions at the individual building scale, yielding sharper boundaries, finer differentiation of functional types, and greater alignment with the underlying urban morphology. For example, in Guangzhou and Zhuhai, GBA-UBF captures small commercial strips embedded within residential areas, which are omitted in EULUC datasets. Similarly, in Hong Kong and Foshan, GBA-UBF reveals detailed spatial organization of public services, educational facilities, and industrial clusters, offering a more realistic and fine-grained portrayal of urban functions.

Fig. 8 shows the 3D view of the representative scenes from six GBA cities. It illustrates precise boundary adherence and clear differentiation among Residential, Commercial, Public Services, Technology & Industry, and Educational & Cultural classes. The

3D visualizations reveal vertical morphology, improving label interpretability and supporting downstream analyses and applications.

We overlay the building footprints with EULUC-China 2.0 [22] function blocks. Each building inherits the function of its corresponding parcel. The results are then consolidated according to the five functional categories defined in this paper, serving as a baseline for comparison. Fig. 9 compares the spatial representation of urban building functions. Compared with EULUC-China 2.0, the proposed dataset preserves semantic consistency with POI distributions and provides building-level precision. This demonstrates that our dataset better reflects the true spatial organization of urban functions while maintaining alignment with real-world patterns.

5.3 Quantitative Comparison

The evaluation of quantitative metrics is shown in Fig. 10. Compared with the EULUC-China 2.0, the GBA-UBF demonstrates a consistently superior performance. Specifically, it achieves markedly higher Top-1 Accuracy, indicating that the majority of building

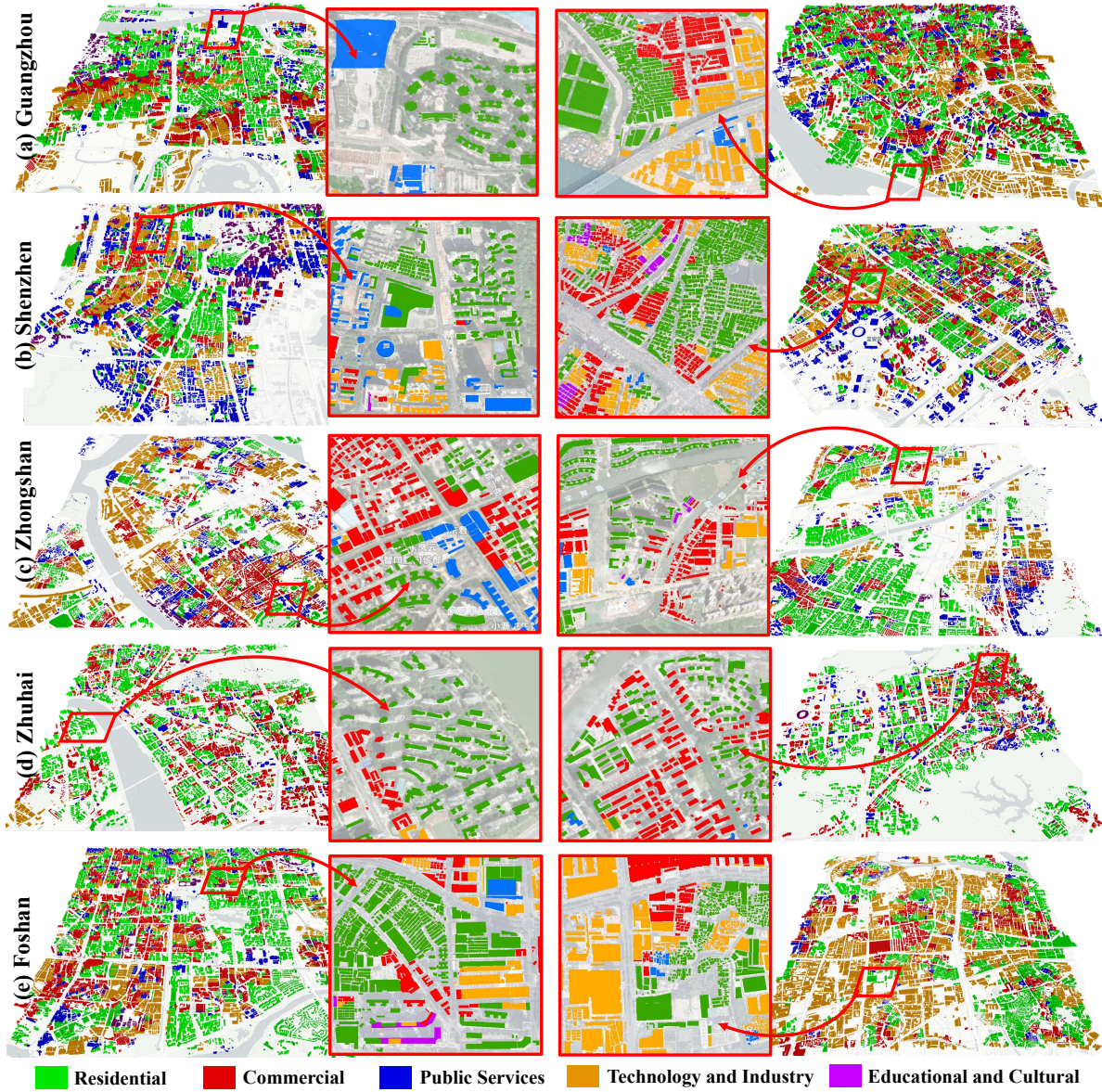


Figure 8: Representative GBA-UBF Dataset 3D Visualization and Corresponding Shapefile Overlay with High-Resolution Remote Sensing Imagery across six cities.

labels directly match the reference categories. It also attains substantially higher Cosine Similarity, reflecting better alignment between predicted distributions and POI-derived spatial probabilities. When integrated into the comprehensive BFMI metric, which balances accuracy and distributional similarity, the GBA-UBF dataset outperforms the EULUC-based baseline by a large margin.

Results indicate that while EULUC-China 2.0 captures dominant building types at the block scale, its granularity remains substantially coarser than our building-level dataset. Because EULUC-China 2.0 is delineated by OpenStreetMap and Tianditu road networks, a single block contains hundreds or even thousands of buildings. As a result, intra-block variation is overlooked, whereas the GBA-UBF dataset provides fine-grained detail at the level of individual buildings. Compared with conventional land use datasets,

the building function dataset developed in this study offers broader applicability and superior precision for fine-scale urban research.

5.4 Field Validation

To further verify the reliability of the Greater Bay Area Building Function Dataset, we conduct field validation in representative urban sites. This validation aims to cross-check the assigned building functions against ground-truth observations collected from photographic evidence.

Fig. 1 illustrates four representative cases. The field validation confirms that the GBA-UBF dataset is capable of distinguishing functionally diverse urban morphologies, even in mixed-use settings. The dataset achieves both semantic interpretability and practical

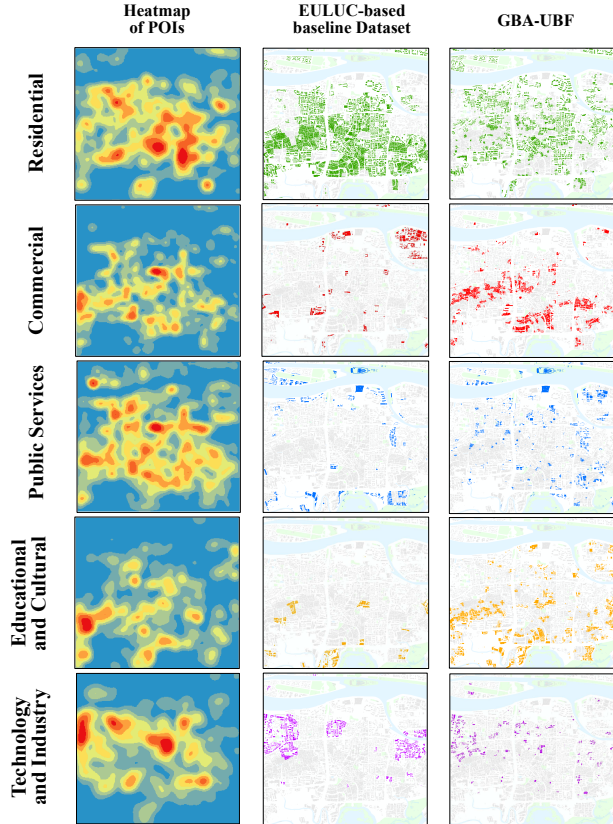


Figure 9: Comparative validation of building function GBA-UBF dataset and land use dataset EULUC-China 2.0 against POI heatmaps.

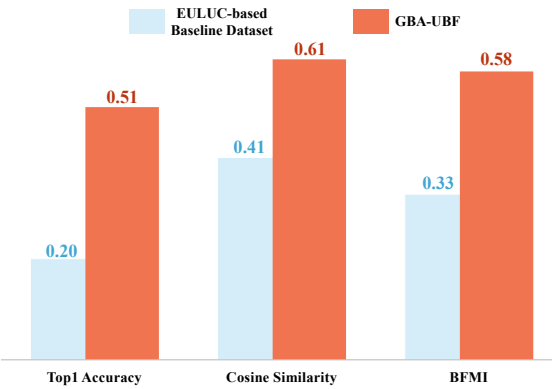


Figure 10: Comparison of Metric Calculations Across Two Datasets.

reliability, offering a robust foundation for urban functional zoning and downstream urban analytics.

5.5 Application Prospects

Prior studies have demonstrated that functional labeling at the scale of individual buildings significantly enhances the accuracy of urban morphology simulations [4]. In flood risk mapping, heterogeneous exposure datasets—such as residential, industrial, and public service categories—serve as essential inputs for high-resolution damage

assessments [41]. In the energy sector, the strong coupling between building functions and energy consumption patterns enables block-level estimation of distributed photovoltaic potential [7]. Similarly, transportation research shows that integrating building functions with travel survey data improves the accuracy of traffic generation rate models by 7–12% [8].

From a planning perspective, local governments urgently require high-resolution (1 m) and near-real-time building-level functional datasets when updating regulatory plans or evaluating the transformation of industrial land. Such detailed building-scale data effectively address the limitations of traditional block-level land-use datasets, which lack the granularity needed for contemporary urban management. Consequently, the dataset developed in this study provides not only methodological innovation but also practical value for diverse urban applications.

5.6 Limitations

This dataset has several limitations. First, the functional classification adopts a “single dominant function” assumption, which overlooks vertical mixed uses, studies in dense cities (e.g., London, New York) show that more than 35% of buildings host multiple functions [11]. Second, POI timeliness and brand changes introduce label drift, estimated at around 8% [20]. Third, the dataset excludes attributes such as building age, floors, and structural type, which are critical for applications such as risk assessment and energy modeling [21]. Finally, limited POI coverage in Hong Kong and Macau leaves 5–10% of buildings in newly reclaimed areas without labels, reducing inference confidence.

6 Conclusion

This paper presents the Greater Bay Area Urban Building Function Dataset (GBA-UBF), a large-scale dataset that assigns five functional categories to nearly four million buildings across six GBA cities. By integrating building footprints, we design a reproducible three-stage pipeline, achieving fine-grained building-level classification and overcoming the limitations of parcel-based land use data.

To validate quality, we introduce the Building Function Matching Index (BFMI), which combines categorical consistency and distributional similarity against POI-derived heatmaps. Comparative experiments with EULUC-China 2.0 show GBA-UBF delivers markedly higher accuracy and better alignment with urban activity patterns, particularly in dense and mixed-use areas. Field validation further demonstrates its semantic reliability and real-world applicability.

GBA-UBF sets a new benchmark for fine-scale urban analytics, bridging the gap between coarse land-use maps and detailed functional mapping. Its building-level granularity supports diverse applications such as digital twins, flood risk assessment, energy modeling, transport analysis, and policy evaluation, thereby advancing both methodological rigor and practical value in urban geoinformatics and remote sensing.

7 Acknowledgments

This work was supported by the National Natural Science Foundation of China under Project 42371343, Guangdong Basic and Applied Basic Research Foundation with Grant No.2024A1515010986.

References

- [1] A. Aidaoui, Y. Chen, and L. Zhang. 2024. Mapping tomorrow's cities: GeoAI strategies for sustainable urban planning and land use optimization. *Journal of Contemporary Urban Affairs* 8, 1 (2024), 158–176.
- [2] Renato Andrade, Ana Alves, and Carlos Bento. 2020. POI mining for land use classification: A case study. *ISPRS International Journal of Geo-Information* 9, 9 (2020), 493.
- [3] Xiaoyong Bian, Chen Chen, Long Tian, and Qian Du. 2017. Fusing local and global features for high-resolution scene classification. *IEEE Journal of Selected Topics in Applied Earth Observations and Remote Sensing* 10, 6 (2017), 2889–2901.
- [4] Filip Biljecki, Joie Lim, James Crawford, Diana Moraru, Helga Tauscher, Amol Konde, Kamel Adouane, Simon Lawrence, Patrick Janssen, and Rudi Stouffs. 2021. Extending CityGML for IFC-sourced 3D city models. *Automation in Construction* 121 (2021), 103440. doi:10.1016/j.autcon.2020.103440
- [5] Bin Chen, Bing Xu, and Peng Gong. 2021. Mapping essential urban land use categories (EULUC) using geospatial big data: Progress, challenges, and opportunities. *Big Earth Data* 5, 3 (2021), 410–441.
- [6] Jun Chen, Jin Chen, Anping Liao, Xin Cao, Lijun Chen, Xuehong Chen, Chaoying He, Gang Han, Shu Peng, Miao Lu, et al. 2015. Global land cover mapping at 30 m resolution: A POK-based operational approach. *ISPRS Journal of Photogrammetry and Remote Sensing* 103 (2015), 7–27.
- [7] Liang Cheng, Fangli Zhang, Shuyi Li, Junya Mao, Hao Xu, Weimin Ju, Xiaoqiang Liu, Jie Wu, Kaifu Min, Xuedong Zhang, and Manchun Li. 2020. Solar energy potential of urban buildings in 10 cities of China. *Energy* 196 (2020), 117038. doi:10.1016/j.energy.2020.117038
- [8] Yan Ling Chi and Hugo Wai Leung Mak. 2021. From Comparative and Statistical Assessments of Liveability and Health Conditions of Districts in Hong Kong towards Future City Development. *Sustainability* 13, 16 (2021). doi:10.3390/su13168781
- [9] Suzanna Cuypers, Andrea Nascetti, and Maarten Vergauwen. 2023. Land use and land cover mapping with VHR and multi-temporal Sentinel-2 imagery. *Remote Sensing* 15, 10 (2023), 2501.
- [10] Runmin Dong, Cong Li, Haohuan Fu, Jie Wang, Weijia Li, Yi Yao, Lin Gan, Le Yu, and Peng Gong. 2020. Improving 3-m resolution land cover mapping through efficient learning from an imperfect 10-m resolution map. *Remote Sensing* 12, 9 (2020), 1418.
- [11] Stephen Evans, Rob Liddiard, and Philip Steadman. 2019. Modelling a whole building stock: domestic, non-domestic and mixed use. *Building Research & Information* 47, 2 (2019), 156–172.
- [12] Cidália C Fonte and Nuno Martinho. 2017. Assessing the applicability of OpenStreetMap data to assist the validation of land use/land cover maps. *International Journal of Geographical Information Science* 31, 12 (2017), 2382–2400.
- [13] Peng Gong, Han Liu, Meinan Zhang, Congcong Li, Jie Wang, Huabing Huang, Nicholas Clinton, Luyan Ji, Wenyu Li, Yuqi Bai, et al. 2019. Stable classification with limited sample: Transferring a 30-m resolution sample set collected in 2015 to mapping 10-m resolution global land cover in 2017. *Sci. Bull.* 64, 6 (2019), 370–373.
- [14] Peng Gong, Jie Wang, Le Yu, Yongchao Zhao, Yuanyuan Zhao, Lu Liang, Zhenguo Niu, Xiaomeng Huang, Haohuan Fu, Shuang Liu, et al. 2013. Finer resolution observation and monitoring of global land cover: First mapping results with Landsat TM and ETM+ data. *International journal of remote sensing* 34, 7 (2013), 2607–2654.
- [15] Ting Han, Jin Ma, Chaolei Wang, Yang Luo, Hongchao Fan, José Marcato, Xinchang Zhang, and Yiping Chen. 2025. CityInsight: Incorporating Dual-Condition based Diffusion Model into Building Footprint Segmentation from Remote Sensing Imagery. *IEEE Transactions on Geoscience and Remote Sensing* (2025).
- [16] Robert Hecht, Gotthard Meinel, and Manfred Buchroithner. 2015. Automatic identification of building types based on topographic databases—a comparison of different data sources. *International Journal of Cartography* 1, 1 (2015), 18–31.
- [17] Anna M Hersperger, Eduardo Oliveira, Sofia Pagliarin, Gaëtan Palka, Peter Verburg, Janina Bolliger, and Simona Grădinaru. 2018. Urban land-use change: The role of strategic spatial planning. *Global Environmental Change* 51 (2018), 32–42.
- [18] Ye Hong and Yao Yao. 2019. Hierarchical community detection and functional area identification with OSM roads and complex graph theory. *International Journal of Geographical Information Science* 33, 8 (2019), 1569–1587.
- [19] Eddie CM Hui, Xun Li, Tingting Chen, and Wei Lang. 2020. Deciphering the spatial structure of China's megacity region: A new bay area—The Guangdong-Hong Kong-Macao Greater Bay Area in the making. *Cities* 105 (2020), 102168.
- [20] Bo Kong, Tinghui Ai, Xinyan Zou, Xiongfeng Yan, and Min Yang. 2024. A graph-based neural network approach to integrate multi-source data for urban building function classification. *Computers, Environment and Urban Systems* 110 (2024), 102094. doi:10.1016/j.compenvurbsys.2024.102094
- [21] Han Li, Hicham Johra, Flavia de Andrade Pereira, Tianzhen Hong, Jérôme Le Dréau, Anthony Maturo, Mingjun Wei, Yapan Liu, Ali Saberi-Derakhshani, Zoltan Nagy, Anna Marszal-Pomianowska, Donal Finn, Shohei Miyata, Kathryn Kaspar, Kingsley Nweye, Zheng O'Neill, Fabiano Pallonetto, and Bing Dong. 2023. Data-driven key performance indicators and datasets for building energy flexibility: A review and perspectives. *Applied Energy* 343 (2023), 121217. doi:10.1016/j.apenergy.2023.121217
- [22] Ziming Li, Bin Chen, Yufei Huang, Han Wang, Yadian Wang, Yiming Yuan, Xueca Li, Jing M Chen, Bing Xu, and Peng Gong. 2025. Enhanced mapping of essential urban land use categories in China (EULUC-China 2.0): integrating multimodal deep learning with multisource geospatial data. *Science Bulletin* (2025).
- [23] Zhuohong Li, Wei He, Mofan Cheng, Jingxin Hu, Guangyi Yang, and Hongyan Zhang. 2023. SinoLC-1: The first 1-meter resolution national-scale land-cover map of China created with the deep learning framework and open-access data. *Earth System Science Data Discussions* 2023 (2023), 1–38.
- [24] Anqi Lin, Xiaomeng Sun, Hao Wu, Wenting Luo, Danyang Wang, Dantong Zhong, Zhongming Wang, Lanting Zhao, and Jiang Zhu. 2021. Identifying urban building function by integrating remote sensing imagery and POI data. *IEEE Journal of Selected Topics in Applied Earth Observations and Remote Sensing* 14 (2021), 8864–8875.
- [25] Baihua Liu, Yingbin Deng, Miao Li, Ji Yang, and Tao Liu. 2021. Classification schemes and identification methods for urban functional zone: A Review of Recent Papers. *Applied Sciences* 11, 21 (2021), 9968.
- [26] Huimin Liu, Yiyuan Xu, Jianbo Tang, Min Deng, Jincai Huang, Wentao Yang, and Fang Wu. 2020. Recognizing urban functional zones by a hierarchical fusion method considering landscape features and human activities. *Transactions in GIS* 24, 5 (2020), 1359–1381.
- [27] Kang Liu, Peiyuan Qiu, Song Gao, Feng Lu, Jincheng Jiang, and Ling Yin. 2020. Investigating urban metro stations as cognitive places in cities using points of interest. *Cities* 97 (2020), 102561.
- [28] Guowei Luo, Jiayuan Ye, Jinfeng Wang, and Yi Wei. 2023. Urban functional zone classification based on POI data and machine learning. *Sustainability* 15, 5 (2023), 4631.
- [29] Ruomu Miao, Yuxia Wang, and Shuang Li. 2021. Analyzing urban spatial patterns and functional zones using sina Weibo POI data: A case study of Beijing. *Sustainability* 13, 2 (2021), 647.
- [30] Hamid Reza Pourghasemi, Mahdis Amiri, Mohsen Edalat, Amir Hossein Ahrary, Mahdi Panahi, Nitheshnirmal Sadhasivam, and Saro Lee. 2020. Assessment of urban infrastructures exposed to flood using susceptibility map and Google Earth Engine. *IEEE Journal of Selected Topics in Applied Earth Observations and Remote Sensing* 14 (2020), 1923–1937.
- [31] Olga Lucia Puertas, Cristian Henríquez, and Francisco Javier Meza. 2014. Assessing spatial dynamics of urban growth using an integrated land use model. Application in Santiago Metropolitan Area, 2010–2045. *Land use policy* 38 (2014), 415–425.
- [32] Wenqi Qiao and Xianjin Huang. 2024. Assessment of the urbanization sustainability and its driving factors in Chinese urban agglomerations: An urban land expansion–Urban population dynamics perspective. *Journal of Cleaner Production* 449 (2024), 141562.
- [33] Xianzheng Shi, Shilei Fu, Jin Chen, Feng Wang, and Feng Xu. 2021. Object-level semantic segmentation on the high-resolution Gaofen-3 FUSAR-map dataset. *IEEE Journal of Selected Topics in Applied Earth Observations and Remote Sensing* 14 (2021), 3107–3119.
- [34] Shivangi Srivastava, John E Vargas-Muñoz, David Swinkels, and Devis Tuia. 2018. Multilabel building functions classification from ground pictures using convolutional neural networks. In *Proceedings of the 2nd ACM SIGSPATIAL international workshop on AI for geographic knowledge discovery*, 43–46.
- [35] Wei Tu, Qingquan Li, Yatao Zhang, and Yang Yue. 2021. User-generated content and its applications in urban studies. In *Urban informatics*. Springer, 523–539.
- [36] Jionghua Wang, Haowen Luo, Wenyu Li, and Bo Huang. 2021. Building function mapping using multisource geospatial big data: a case study in Shenzhen, China. *Remote Sensing* 13, 23 (2021), 4751.
- [37] Hao Wu, Anqi Lin, Keith C Clarke, Wenzhong Shi, Abraham Cardenas-Tristan, and Zhenfa Tu. 2021. A comprehensive quality assessment framework for linear features from Volunteered Geographic Information. *International Journal of Geographical Information Science* 35, 9 (2021), 1826–1847.
- [38] Hao Wu, Anqi Lin, Xudong Xing, Danxia Song, and Yan Li. 2021. Identifying core driving factors of urban land use change from global land cover products and POI data using the random forest method. *International Journal of Applied Earth Observation and Geoinformation* 103 (2021), 102475.
- [39] Shuping Xiong, Xiuyuan Zhang, Haoyu Wang, Yichen Lei, Ge Tan, and Shihong Du. 2025. Mapping the first dataset of global urban land uses with Sentinel-2 imagery and POI prompt. *Remote Sensing of Environment* 327 (2025), 114824.
- [40] Di Yang, Chiung-Shiu Fu, Audrey C Smith, and Qiang Yu. 2017. Open land-use map: a regional land-use mapping strategy for incorporating OpenStreetMap with earth observations. *Geo-spatial information science* 20, 3 (2017), 269–281.
- [41] Insang Yu, Kiyong Park, and Eui Hoon Lee. 2021. Flood Risk Analysis by Building Use in Urban Planning for Disaster Risk Reduction and Climate Change Adaptation. *Sustainability* 13 (11 2021), 13006. doi:10.3390/su132313006
- [42] Daniele Zanaga, Ruben Van De Kerchove, Dirk Daems, Wanda De Keersmaecker, Carsten Brockmann, Grit Kirches, Jan Wevers, Oliver Cartus, Maurizio Santoro, Steffen Fritz, et al. 2022. ESA WorldCover 10 m 2021 v200. (2022).

- [43] Xiuyuan Zhang, Shihong Du, and Qiao Wang. 2017. Hierarchical semantic cognition for urban functional zones with VHR satellite images and POI data. *ISPRS Journal of Photogrammetry and Remote Sensing* 132 (2017), 170–184.
- [44] Xiaoyi Zhang, Wenwen Li, Feng Zhang, Renyi Liu, and Zhenhong Du. 2018. Identifying urban functional zones using public bicycle rental records and point-of-interest data. *ISPRS international journal of geo-information* 7, 12 (2018), 459.
- [45] Xiao Zhang, Liangyun Liu, Tingting Zhao, Wenhan Zhang, Linlin Guan, Ming Bai, and Xidong Chen. 2025. GLC_FCS10: a global 10-m land-cover dataset with a fine classification system from Sentinel-1 and Sentinel-2 time-series data in Google Earth Engine. *Earth System Science Data Discussions* 2025 (2025), 1–27.
- [46] Chen Zhong, Xianfeng Huang, Stefan Müller Arisona, Gerhard Schmitt, and Michael Batty. 2014. Inferring building functions from a probabilistic model using public transportation data. *Computers, Environment and Urban Systems* 48 (2014), 124–137.
- [47] Qi Zhou, Shuzhu Wang, and Yaoming Liu. 2022. Exploring the accuracy and completeness patterns of global land-cover/land-use data in OpenStreetMap. *Applied Geography* 145 (2022), 102742.
- [48] Li Zhuo, Qingli Shi, Chenyang Zhang, Qiuping Li, and Haiyan Tao. 2019. Identifying building functions from the spatiotemporal population density and the interactions of people among buildings. *ISPRS International Journal of Geo-Information* 8, 6 (2019), 247.